

J. agric. Sci., Camb. (1984), **102**, 371–382

With 7 text-figures

Printed in Great Britain

371

A winter wheat crop simulation model without water or nutrient limitations

By A. H. WEIR*, P. L. BRAGG†§, J. R. PORTER‡ AND J. H. RAYNER*

* Rothamsted Experimental Station, Harpenden, Herts., AL5 2JQ

† Agricultural Research Council Letcombe Laboratory, Wantage, Oxfordshire, OX12 9JT

‡ Long Ashton Research Station, University of Bristol, Long Ashton, Bristol, BS18 9AF

(Revised MS. received 18 August 1983)

SUMMARY

A whole crop computer simulation model of winter wheat has been written in FORTRAN and used to simulate the growth of September- and October-sown crops of Hustler wheat at Rothamsted for the years 1978–9, 1979–80 and 1980–1. Results of the simulations, which are for crops with adequate water and nutrients, are compared with observations from experiments at Rothamsted. The model uses daily maximum and minimum temperatures and daylength to calculate the dates of emergence, double ridge, anthesis and maturity of the crops and the growth and senescence of tillers and leaves. In the simulations, the canopy intercepts daily radiation and produces dry matter that is partitioned between roots, shoots, leaves, ears and grain. Partial simulations, using observed LAI values, produced dry matter in close agreement with observations of late-sown crops, but consistently overestimated the total dry-matter production of the early-sown crops. Full simulation described satisfactorily the average difference in dry-matter production to be expected with changes in time of sowing, but did not give as close correspondence for individual crops. A grain growth submodel, that linked maximum grain weight to average temperatures during the grain growth period, correctly simulated the observed growth of individual grains in the 1981 crop. The benefits to be obtained by combining whole crop modelling with detailed crop observations are discussed.

INTRODUCTION

The construction of this model, which we call ARCWHEAT 1, is a collaborative project between four Institutes supported by the Agricultural Research Council: Letcombe Laboratory, Long Ashton Research Station, Plant Breeding Institute, Cambridge, and Rothamsted Experimental Station. The long-term aim is to develop a mechanistic simulation model of the growth of winter wheat that can be used to emphasize areas where research into growth processes is needed, to explain differences in yields from field experiments in terms of sites and seasons, and to estimate yield differences attributed to the effects of soil and weather throughout the United Kingdom.

Whole-crop modelling has increased greatly in the past few years with notable contributions by Thornley (1976), De Wit *et al.* (1978), Milthorpe &

Moorby (1979), and Penning de Vries & Van Laar (1982). Wheat models have been produced by Morgan (1976) and Hochman (1979), by the Wageningen school and by Ritchie and co-workers at Temple, Texas. The principles of the ARC model were described by Landsberg & Porter (1982) and Porter *et al.* (1983). This model has now been developed to the point at which it can simulate the growth of healthy crops with adequate nutrients for different sowing dates and seasons. In this form the only driving variables are radiation and temperature. This paper describes the model and compares the results of simulations with observations of the growth of six experimental crops.

THE MODEL

ARCWHEAT 1, shown diagrammatically in Fig. 1, consists of five submodels: phenological development, tiller and leaf production, root production,

§ Present address: Heyden Datasystems, London, NW4 2JQ.

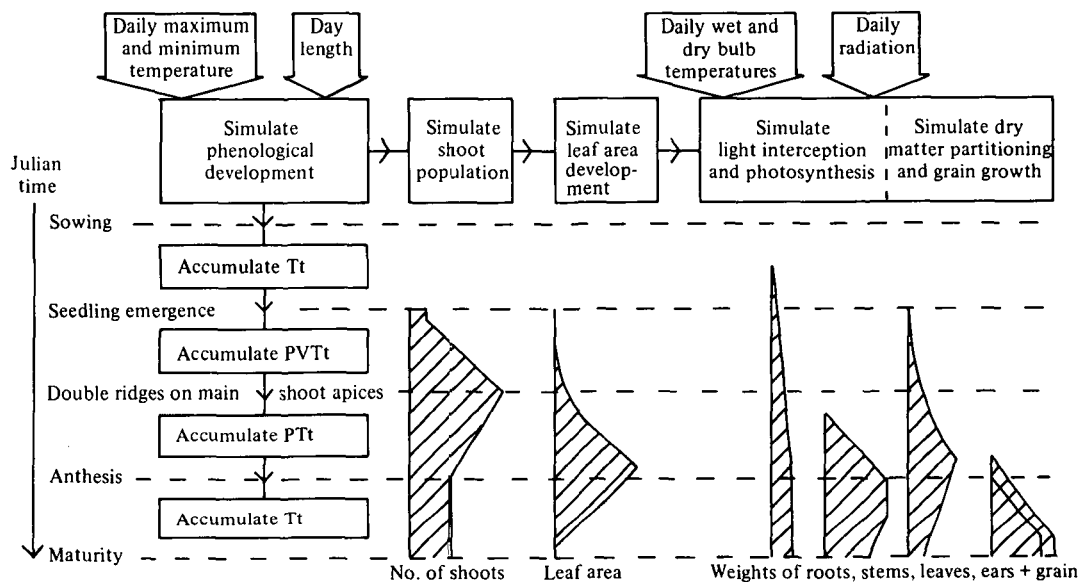


Fig. 1. Diagrammatic representation of the wheat computer model showing the interaction between the submodels: phenological development, tiller and leaf growth, root growth, light interception and photosynthesis, dry-matter partitioning and grain growth. The arrowed boxes show the driving variables. Tt, thermal time; PTt, thermal time modified by photoperiod; PVTt, thermal time modified by photoperiod and vernalization. For details, see the text.

light interception and photosynthesis, dry-matter partitioning and grain growth.

Phenological development submodel

The submodel is given sowing date, site latitude and daily maximum and minimum temperatures, and calculates the dates of occurrence of the development stages: seedling emergence, appearance of double ridges on the main shoot apex, anthesis and maturity. Maturity is chosen to represent the state of experimental crops at hand-harvest date.

Four types of thermal time ($^{\circ}\text{C}$ days for a function of maximum and minimum temperature) are used. For the phase from sowing to emergence thermal time is calculated using a base temperature of 1°C . From emergence to double ridges this thermal time is modified by vernalization and photoperiod factors and for the phase from double ridges to anthesis by photoperiod only. From anthesis to maturity, thermal time is calculated assuming a base temperature of 9°C . Calculation of thermal time of the first three phases uses the method of Gallagher and Lumsden (Lumsden, 1980; Gallagher, Thorne & Taylor, 1981). Lumsden (1980) chose the base temperature of 1°C and other parameters used in the photoperiodic and vernalization responses of the crop from consideration of the development of wheat crops grown at Rothamsted and Sutton Bonington in the period 1974–8. The base temperature of the

last phase is based on the analyses shown in Fig. 2 using unpublished data of G. N. Thorne and P. J. Welbank.

Thermal time. This is obtained as the sum of eight contributions each day of a cosinusoidal varia-

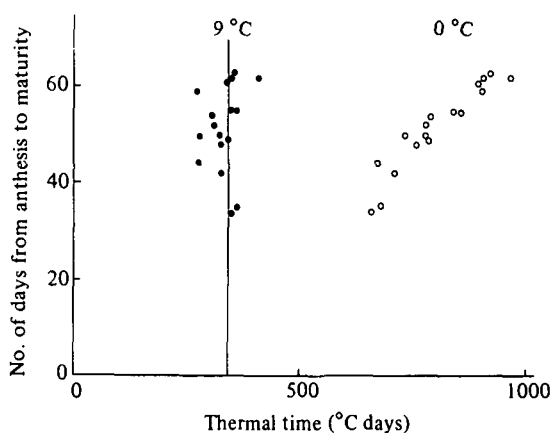


Fig. 2. Number of days from anthesis to maturity plotted against thermal time totals above base temperatures of 0°C (\circ) and 9°C (\bullet). The straight line through 340 $^{\circ}\text{C}$ days was fitted by eye. Unpublished crop data for Cappelle-Desprez, Maris Huntsman, Flanders and Hustler winter wheat over the seasons 1972–82 supplied by G. N. Thorne and P. J. Welbank.

tion between the observed maximum and minimum temperatures:

$$Tt = \frac{1}{8} \sum_{r=1}^{r=8} [T_H - T_{base}] \text{ } ^\circ\text{C days} \quad (1)$$

where $T_H = T_{min} + f_r (T_{max} - T_{min}) \text{ } ^\circ\text{C}$ (2)

and $f_r = \frac{1}{2}[1 + \cos \frac{2\pi}{8} (2r - 1)]$ (3)

T_H , T_{base} , T_{max} and T_{min} are in $^\circ\text{C}$; negative contributions are treated as zero.

There are reduced contributions for 1/8-day temperatures above 26 $^\circ\text{C}$ (T_{opt}) falling to zero at 37 $^\circ\text{C}$ (TD_{max}) (Arndt, 1945). At T_{opt} the contribution $T_H - T_{base}$ is $T_{opt} - T_{base}$ $^\circ\text{C}$. Between T_{opt} and TD_{max} the contribution becomes $(T_{opt} - T_{base}) (TD_{max} - T_H) / (TD_{max} - T_{opt})$ $^\circ\text{C}$.

Photoperiod effects. The number of photoperiod-effective hours (P_H) (after Francis, 1970) is calculated for each day. If a day has 20 or more photoperiod-effective hours, thermal time is not reduced, but if it has fewer, thermal time is proportionally reduced by multiplication by a photoperiod factor (FP).

P_H is calculated from site latitude (Lat) and Julian day number (Jday) using formulae describing the relative movement of the earth and sun. The angle of the sun above the equator (Dec) is given by

$$\text{Dec} = \sin^{-1} (0.3978 \sin \theta) \text{ rad}, \quad (4)$$

where $\theta = \theta_1 + \theta_2$ rad (5)

and $\theta_1 = 2\pi (Jday - 80) / 365$ rad (6)

and $\theta_2 = 0.0335 (\sin 2\pi Jday - \sin 2\pi 80) / 365$ rad. (7)

Photoperiod-effective radiation for each day begins and ends when the sun is 6 $^\circ$ (0.10453 rad) below the horizon.

Then if $D = -0.10453 / \cos \text{Lat} \cdot \cos \text{Dec}$ (8)

and $P_R = \cos^{-1} (D - \tan \text{Lat} \cdot \tan \text{Dec})$ rad, (9)

$$P_H = 24P_R / \pi \text{ hours}, \quad (10)$$

$$\text{FP} = (P_H - P_{base}) / (P_{opt} - P_{base}). \quad (11)$$

Gallagher and Lumsden set P_{opt} at 20 h and limited FP to vary between 0 and 1. Thus FP can reduce, but not increase, the accumulation of thermal time. They also set P_{base} to 0 h for the phase from emergence to double ridge, but to 7 h from double ridge to anthesis. These settings have been retained.

Vernalization. The vernalization factor used to modify thermal time in the growth phase between emergence and double ridges depends on the temperature history of the plant summarized as

cumulative vernalized day degrees (VDD). VDD accumulates from time of germination, although the factor (FV) derived from it modifies thermal time only after emergence. If T_{max} exceeds 30 $^\circ\text{C}$ for any day, half the VDD accumulated up to that time is lost.

To calculate VDD and FV, temperatures are obtained from equations (2) and (3) by putting $r = 1 \dots 8$ and are used to derive vernalization effectiveness factors (V_{eff})

for T_H values of 3–10 $^\circ\text{C}$ $V_{eff} = 1$, (12)

for T_H values of –4–3 $^\circ\text{C}$ $V_{eff} = (T_H + 4) / 7$, (13)

for T_H values of 10–17 $^\circ\text{C}$ $V_{eff} = (17 - T_H) / 7$. (14)

Thus full vernalization is obtained between 3 and 10 $^\circ\text{C}$ and reduced amounts between –4 and 3 $^\circ\text{C}$ and 10 and 17 $^\circ\text{C}$. Cumulative vernalization is given by summing all the 1/8 day contributions

$$\text{VDD} = \sum_{i=1}^{i=n} \frac{1}{8} \sum_{r=1}^{r=8} V_{eff} \text{ vernal days}, \quad (15)$$

where i is the day number and n the number of days from germination. The vernalization factor (FV) is given by

$$\text{FV} = (\text{VDD} - V_{base}) / (V_{sat} - V_{base}). \quad (16)$$

Gallagher and Lumsden (Lumsden, 1980) set V_{sat} at 33 and V_{base} at 8 vernal days and normalized FV between 0 and 1. As with FP their values have been retained unchanged. In the calculation of photovernalized thermal time, PVTt, the daily thermal time contribution is multiplied by both FP and FV.

Appendix Table 1 shows the base temperatures and thermal time totals used for Hustler wheat.

Tiller and leaf growth submodel

Details of the simulation of tiller and leaf growth are given in an accompanying paper (Porter, 1984). In this submodel a given population of main stems grows tillers on a weekly basis using a tiller production rate and the accumulated thermal time of the previous week. Tiller production ceases at the double ridge stage and is succeeded by tiller death in which the latest formed tillers have the greatest probability of dying. Tillers surviving at anthesis are considered to develop ears.

Leaves appear on main shoots and tillers at intervals determined by thermal time and the rate of change of daylength at emergence. Leaf durations and maximum sizes are functions of leaf number. Thus the submodel generates a population of ear-bearing stems and a canopy of green leaves that is a function of the number of stems and the number and sizes of their surviving leaves.

Root growth submodel

In this submodel each plant grows five seminal roots at a linear rate that is modified by the daily mean air temperature and availability of assimilate (Porter *et al.* 1983). The specific weight of seminal roots is set to 1.5×10^{-4} g/cm, and the temperature-related growth rate factor, TR, is given by

$$\text{TR} = 0.2 + 0.12 T, \quad (17)$$

where T °C is the daily mean temperature. A surplus of assimilate over that required for seminals is used to grow lateral roots, which have a specific weight of 4×10^{-5} g/cm. Thirty per cent of the assimilate available is retained in each layer and the remainder passed to the layer below. Thus the amount of lateral root per layer decreases exponentially with depth down to the limit of penetration of the seminal roots.

Light interception and photosynthesis submodel

The amount of photosynthetically active radiation (PAR) falling on each square metre of crop is calculated from daily values of net short-wave energy incident at crop height. These are combined with values of green leaf area index (LAI) obtained from the tiller and leaf growth submodel to obtain incident PAR each hour at the mid-points of each leaf area layer, using a radiation interception model similar to that of Charles-Edwards (1978). The amounts of CO₂ fixed per layer/hour as photosynthate are then calculated using the photosynthesis equations of Marshall & Biscoe (1980*a, b*). A modification, after Tenhunen, Yocum & Gates (1976), varies the rate of photosynthesis with temperature. The total photosynthate produced during the hours of daylight is reduced by amounts lost to growth respiration and maintenance respiration, calculated according to McCree (1974), to give the assimilate produced each day.

Radiation interception. If Q_p is the PAR at the top of the canopy, then the intensity of PAR at level z ($Q_p(z)$) in the canopy is given by

$$Q_p(z) = \frac{Q_p \cdot k}{(1-m)} \exp[-k \cdot \text{LAI}(z)] \quad \text{W/m}^2, \quad (18)$$

where $\text{LAI}(z)$ is the green leaf area index at level z with $z = 0$ at the top of the canopy, k is an extinction coefficient and m a leaf transmission coefficient for PAR.

Photosynthesis. The rate of photosynthesis, net of photorespiration, P_p (mg CO₂/m² per sec), is obtained from the quadratic equation fitted to the photosynthesis-light response curve of Marshall &

Biscoe (1980*a*). It is the same as equation (5) of Thornley (1976, p. 94) with $\theta = 0.995$

$$0.995 P_p^2 - P_p(P_{\text{max}} + \alpha Q_p(z)) + \alpha Q_p(z) P_{\text{max}} = 0, \quad (19)$$

α (mg/J) is the photosynthetic efficiency. The maximum photosynthesis rate, P_{max} , is given by

$$P_{\text{max}} = 0.995 C_a / r_p \quad \text{mg/m}^2 \text{ per sec}, \quad (20)$$

where C_a (mg/m³) is the ambient CO₂ concentration and r_p is the total physical resistance to CO₂ diffusion.

$$r_p = r_a + r_s + r_m \quad \text{sec/m}, \quad (21)$$

where the crop boundary layer resistance, r_a , and the mesophyll resistance, r_m , have fixed values and the stomatal resistance, r_s , has the form

$$r_s = 1.56 \times 75 (1 + 100/Q_p(z)) (1 - 0.3D) \text{sec/m}, \quad (22)$$

where D (kPa) is the vapour pressure deficit. In this model the crop is considered to be free from water stress and thus r_s is not affected by leaf water status.

Values of P_p , obtained by solving equation (18) for each unit leaf area layer and part layer for each daylight hour, are summed to give the gross amount of CO₂ transformed to carbohydrate each day.

Temperature correction of maximum photosynthetic rate. Low temperatures limit the maximum photosynthetic rate at saturating light and CO₂ concentrations (Tenhunen, Weber, Yocum & Gates, 1976). The temperature-dependent maximum photosynthetic rate (P_m) is given by

$$P_m = \frac{0.044 \times 6 \times 10^9 T(k) \exp(-\Delta H_1/RT(k))}{1 + \exp(-\Delta H_2/RT(k)) \exp(\Delta S/R)} \quad \text{mg/m}^2 \text{ per sec}, \quad (23)$$

where $T(k)$ is leaf temperature in degrees Kelvin, ΔH_1 and ΔH_2 (cal/mol) are the activation and denaturation energies for the electron transport system, R (cal/K per mol) is the gas constant, and ΔS (cal/K per mol) is the entropy change on denaturation of the electron transport system. This modifies the photosynthesis equation, as follows:

$$0.995 \frac{P_p^2}{P_{\text{max}}} \left\{ \frac{1}{\alpha Q_p(z)} + \frac{1}{P_m} \right\} - P_p \left\{ \frac{1}{\alpha Q_p(z)} + \frac{1}{P_m} + \frac{1}{P_{\text{max}}} \right\} + 1 = 0. \quad (24)$$

Respiration. Total respiration, R , is calculated daily as the sum of growth and maintenance respiration. Growth respiration is a fixed fraction of the hourly values of photosynthate production, P_p , summed over daylight hours and expressed as

CH₂O equivalent ($P_g(\text{CH}_2\text{O}) = 0.65P_g(\text{CO}_2)$). Maintenance respiration is temperature sensitive (McCree, 1974) and is a fraction, changed after anthesis, of the whole crop weight

$$R = 0.65 a \sum_{h=0}^H P_g(h) + Wb2^{0.05(T_{\max} + T_{\min})}$$

g/m² per day, (25)

where *a* is the growth respiration coefficient, *H* the number of daylight hours, *W* (g/m²) the crop weight and *b* the maintenance respiration coefficient.

Dry-matter partitioning and grain growth submodel

Daily net photosynthate production, $P_n(\text{CH}_2\text{O})$, calculated as the difference between daily photosynthate production and respiration

$$P_n(\text{CH}_2\text{O}) = P_g(\text{CH}_2\text{O}) - R \quad \text{g/m}_2 \text{ per day} \quad (26)$$

is divided between roots, leaves and stems, and later, ears. The proportions of dry matter allocated to stems, leaves and roots change in a preset manner at double ridge, anthesis and maturity (see Appendix Table 1). Ear growth occurs during the last 400 PTt °C days before anthesis; during ear growth 30% of new net assimilate is allocated to

the ears. Following R. A. Fischer (personal communication), the number of grains per ear is determined from ear weight at anthesis by assuming that each 10 mg of ear weight is equivalent to one grain.

Grain growth is modelled by making all the net assimilate produced between anthesis and maturity available for grain growth, together with an assimilate pool of 30% of shoot weight at anthesis (Austin *et al.* 1977). It is assumed that chaff weight at maturity is equal to ear weight at anthesis (Pearman, Thomas & Thorne, 1977; Martinez-Carrasco & Thorne, 1979). The phase from anthesis to maturity is divided 55:240:55 in thermal time into three grain growing periods: initiation, linear growth and mature. During the initiation period all net assimilate accumulates in the pool. During the mature period grain does not increase in weight, but if daily net assimilate is negative it loses weight proportionately to the other plant parts. During the linear period grain growth has a temperature-limited maximum growth rate, G_{\max} (Spiertz, 1977),

$$G_{\max} = 0.045 (T_{\max} + T_{\min})/2 + 0.4 \quad \text{mg/grain per day.} \quad (27)$$

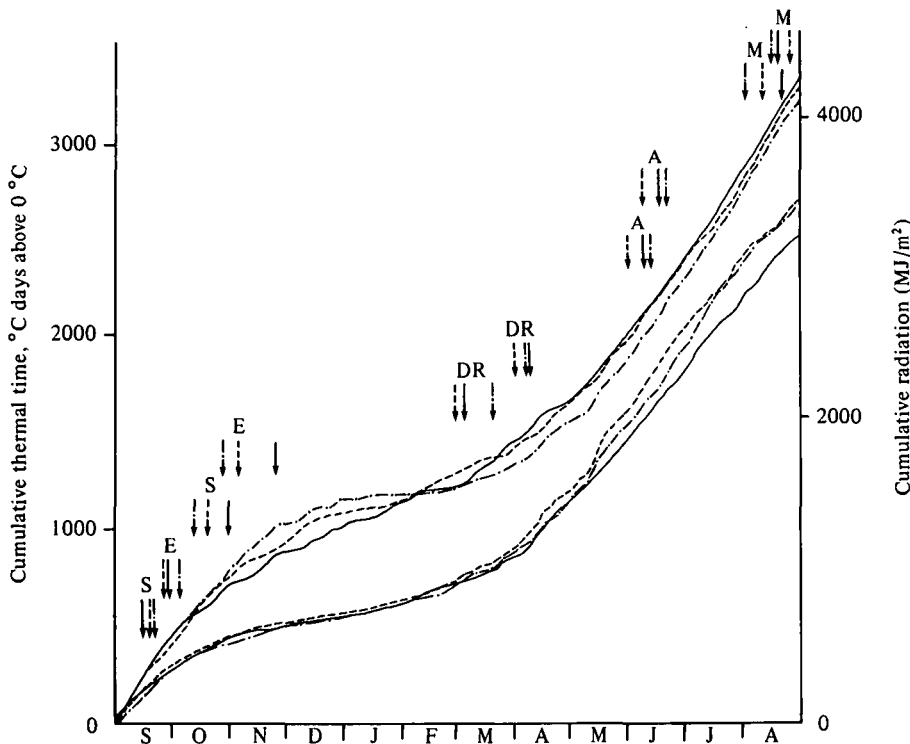


Fig. 3. Cumulative thermal time (above) and cumulative radiation (below) for the three growing seasons of 1978-9 (—), 1979-80 (---) and 1980-1 (.....). Arrows indicate dates of sowing S, emergence E, double ridges DR, anthesis A and maturity M.

Table 1. Observed and computer-simulated dry matter weights and yield components for *Husler* winter wheat grown at Rothamsted in 1978-81

		1979		1980		1981		Means	
		E	L	E	L	E	L	E	L
Top weight, anthesis (g/m ²)	Observed mean	1147	1177	1197	921	1196	1071	1180	1056
	s.e.	30.6		12.1		13.2		20.5	
	Simulated 1	1223	1150	1386	1002	1209	1088	1273	1080
	Simulated 2	1256	936	1384	859	1209	844	1283	879
Top weight, maturity (g/m ²)	Observed mean	1706	1663	1800	1540	2010	1780	1839	1661
	s.e.	24.1		13.4		26.2		22.0	
	Simulated 1	1960	1809	1965	1512	1910	1791	1945	1704
	Simulated 2	2058	1575	2232	1523	2015	1473	2101	1523
Grain yield (g/m ²)	Observed mean	846	837	837	771	823	770	835	793
	s.e.	12.2		7.4		10.7		10.3	
	Simulated 1	862	838	934	750	870	869	889	819
	Simulated 2	843	746	1127	833	895	773	955	784
Harvest index (%)	Observed mean	50	50	47	50	41	43	45	48
	s.e.	1.4		0.8		1.1		1.2	
	Simulated 1	44	46	48	50	46	49	46	48
	Simulated 2	41	47	50	55	44	52	45	51
No. of grains/m ² ($\times 10^3$)	Observed mean	21.3	20.9	20.4	19.3	21.3	20.6	21.0	20.3
	s.e.	1.01		0.55		0.86		0.83	
	Simulated 1	23.2	22.3	25.6	21.8	22.3	21.9	23.7	22.0
	Simulated 2	22.8	20.0	26.9	20.5	22.9	19.8	24.2	20.1
No. of ears/m ²	Observed mean	620	622	543	476	542	556	568	551
	s.e.	14.5		7.1		9.6		10.8	
	Simulated 2	655	616	635	576	601	627	630	606
No. of grains/ear	Observed mean	34.4	33.6	37.5	40.5	39.3	37.1	37.1	37.1
	s.e.	0.84		0.54		0.89		0.77	
	Simulated 2	34.8	32.5	42.4	35.6	38.1	31.6	38.4	33.2
Grain weight (mg/ grain)	Observed mean	40.2	40.3	41.7	40.3	39.2	37.5	40.4	39.3
	s.e.	0.52		0.24		0.47		0.43	
	Simulated 2	37.0	37.3	41.9	40.6	39.1	39.0	39.5	39.0
Grain pool, g/m ² , simulated 2, at anthesis		322	223	337	210	298	196	319	210
	at maturity	258	103	57	7	215	49	177	52
Root weight, g/m ² , simulated 2, at anthesis		271	177	267	156	234	140	257	158

E and L, early-sown and late-sown crops.

s.e. is the pooled standard error of the means of 32 plots for 1980, 16 plots for 1979 and 1981.

Simulated 1 is for computer simulations using observed LAI values, Simulated 2 for calculations using simulated LAI values.

Grains grow at the maximum rate unless limited by the availability of daily and pool assimilate.

RESULTS AND DISCUSSION

Observed weather and crop data

The six crops used to test the model came from the early- and late-sown treatments of the multi-factorial wheat experiments at Rothamsted in the seasons 1978-9, 1979-80 and 1980-1.

Weather. Figure 3 summarizes the weather for the three seasons in terms of cumulative radiation and cumulative mean temperature, the data being taken from the meteorological station records. Cumulative temperatures of about 1000 day-degrees were reached at dates about 40 days apart in the winters of 1978-9 and 1980-1. Through the spring and early summer 1979 lagged the other years by about 10 days. July 1980 was cooler than in the other 2 years, leading to a longer grain-filling

period for the two 1980 crops. Solar radiation was very similar during the three winters, but 1981 was duller from the beginning of April onwards, so that during the period of rapid growth to the end of July 1981 the crops received about 8% less radiation.

Test crops. The predictions of the model were compared with observations made on the early and later sown treatments of the multifactorial experiments on Hustler winter wheat made at Rothamsted in 1978–9, 1979–80 and 1981–1 (Prew *et al.* 1983; Thorne *et al.* 1981, 1982). Mean values for the two sowing dates, averaged over all other treatments, were used except when pests or diseases were known to have reduced growth. When this occurred means from the plots treated with the appropriate pesticide were used. Hence in all years the data for the last two samplings are from plots given fungicide and, in 1979, aphicide. Data for the crops in 1981 from the March sampling onwards were taken from plots given aldicarb. As a result of this selection, and of variation in the number of plots sampled on the different occasions, the number of plots included in the means quoted below was either 16 or 32. All the means quoted are averages of all the nitrogen treatments tested and, after irrigation started, of the two irrigation treatments. Nitrogen and irrigation had only small effects on grain yield although larger ones on some aspects of growth. These have been ignored in this paper. The sampling procedure ensured that stem bases were included in estimates of above ground crop until April, but not from May onwards when crop samples were cut at ground level. The figures quoted in this paper for these later samplings include a correction for the stem bases estimated as 50 g/m² at maturity and anthesis but reduced proportionately to top weight for the May sampling. The grain yields quoted are for hand harvest samples.

The figures for leaf area index given here and by Porter (1984) include the area of green sheath estimated as height × diameter. In the original publications sheath area was estimated as height × circumference.

The mean weights of the above-ground crops (top weights) for the 3 years of the early- and of the late-sown crops increased from 1180 and 1056 g/m² at anthesis to 1839 and 1661 g/m² at harvest (Table 1), increases of 659 and 605 g/m². Grain weights were 835 and 793 g/m², 176 and 188 g/m² more than the additional dry weight gains made during the grain-filling periods. This extra weight, which represents 20 and 23% of stem and leaf weights at anthesis, was supplied from a carbohydrate pool temporarily stored in the upper stems and leaves. The early-sown crops were about 5% heavier in grain yield and 11% in top weight than

the late-sown, the harvest index, the ratio of grain weight to total top weight, being 45 and 48% for the two groups.

When considering individual years, the 1980E crop had the largest top weight at anthesis and 1981E at maturity, and 1980L the smallest, but these differences were not maintained in the grain yields, which were very similar for all six crops. Variation in number of ears tended to be compensated for by number of grains per ear, so that number of grains per unit area of ground showed little variation. The range of top weights at anthesis was 25%, and at harvest 27%, of the mean of the six crops. Number of grains per square metre had a range of 10% of the mean and grain yield a range of 9%.

Simulated crops

It was our intention to use published crop data to develop the model and test its performance by comparing simulation runs against the observed crop data from the WW/3 experiments. This did not prove entirely possible, however, because of the lack of alternative crop data on Hustler winter wheat. Thus, the values of 0.002 and 0.001 used for the maintenance respiration coefficient (Appendix Table 1) were modified from that of 0.003 for young clover plants (McCree, 1974) to represent more closely the reduced respiration of wheat crops, as deduced from the observed average growth rates of the six test crops. Similarly, the general scheme of partitioning of assimilate as given by R. A. Fischer (personal communication) was modified to conform to the mean weights of the different parts of the test crops.

Phenological development. Five development stages of the observed crops are shown in Fig. 3 and again, contrasted with the simulated crops, in Fig. 4. Figure 4 shows how the observed interval from sowing to emergence increased with the lateness of sowing from 6 to 24 days. This interval was simulated on average to within 2 days, with individual crops ranging from 0 to 6 days. The time from emergence to double ridges, a stage that is difficult to observe closer than to 3 or 4 days, varied from 138 to 167 days. In 1979 and 1980 these intervals for the early- and late-sown crops differed by only 3 and 4 days, but in 1981 by 20 days. Simulation of the interval was correct to within 5 days on average, with individual crops ranging from 2 to 10 days. The interval between emergence and double ridges shortens with increased lateness of sowing and this trend continues in the next phase up to anthesis, so that the occurrence of 50% anthesis for the six crops spanned only 19 days, from 11 to 30 June, compared with 58 days for emergence, from 26 September to 23 November. The interval from double ridges to anthesis was simulated to

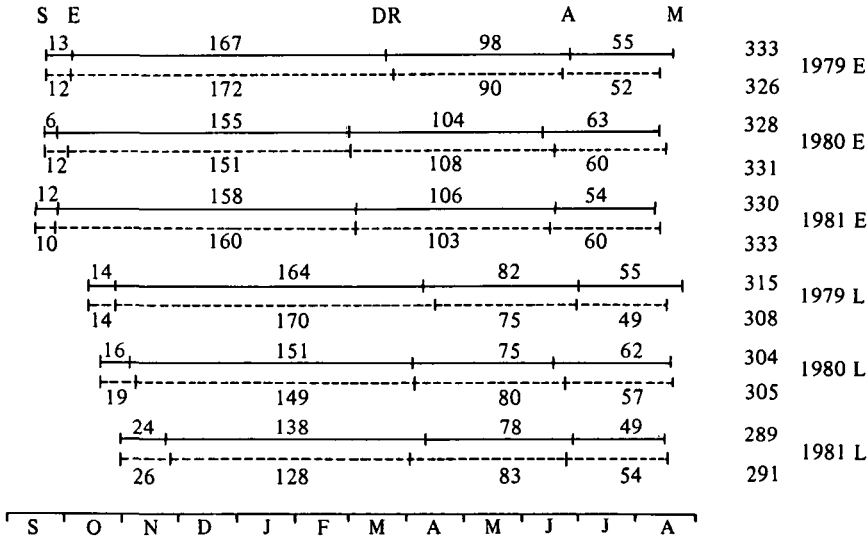


Fig. 4. Diagram showing the timing of phenological development stages for observed (—) and simulated (---) wheat crops. S, sowing; E, emergence; DR, double ridge; A, anthesis; M, maturity. The numbers indicate phase durations, in days.

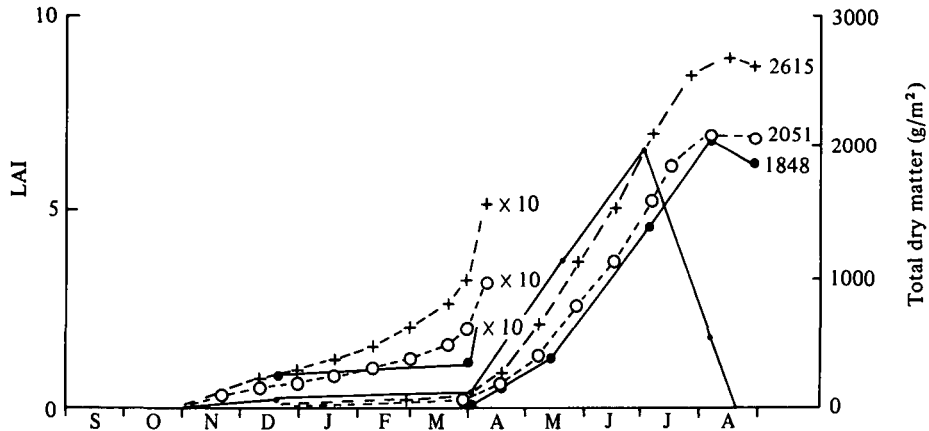


Fig. 5. Diagram showing the changes in observed LAI with time of the 1979L wheat crop (—), the observed total dry-matter values (●—●), and simulated total dry-matter values using the observed LAI with temperature-modified photosynthesis (○--○) and without temperature modification (+--+).

within 5 days on average, the range being 3–8 days. The observed period from anthesis to maturity varied from 49 to 63 days. The longest grain-filling periods were for the early- and late-sown crops in the cool summer of 1980. The simulated intervals varied from 49 to 60 days, a slightly smaller range than that observed. Thus the use of a rather high base temperature of 9 °C did not cause overestimation of the differences between crops.

Dry-matter production and partitioning. Figure 5 shows the observed LAI and dry-matter variations

with time of the 1979L crop, together with simulated dry-matter changes using unmodified and temperature-modified photosynthesis. The unmodified photosynthesis gives weight increases that are 30–40% greater than observed. The simulation using temperature-modified photosynthesis slightly exceeded the observed crop dry matter during the winter and continued to do so up to the maximum on 6 August, when the difference was only 45 g/m². The difference between the two then increased to 190 g/m² at maturity owing to differ-

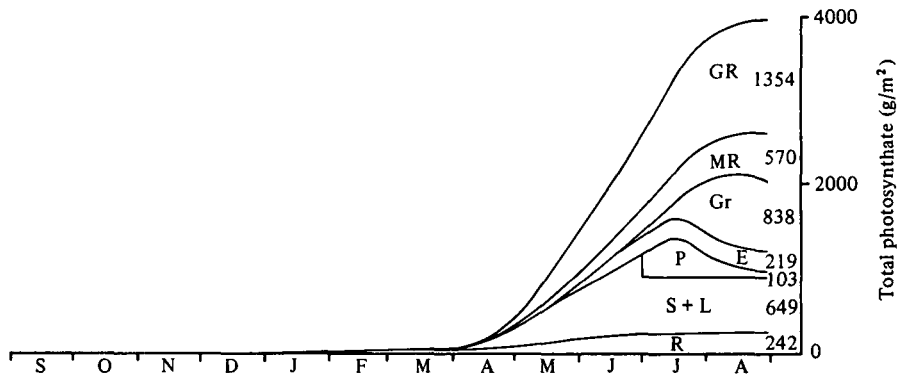


Fig. 6. Changes with time in total photosynthate, net of photorespiration, and its partitioning for the simulated 1979L crop with observed LAI and temperature-modified photosynthesis. GR, growth respiration; MR, maintenance respiration; Gr, grain; E, ears; P, pool of photosynthate for grain growth; S + L, stems and leaves; R, roots.

ences in respiration of the simulated and observed crops.

Figure 6 shows the changes with time of production of total photosynthate, net of photorespiration, of the same simulation as in Fig. 5. The amounts of respired CO_2 and thus of residual dry matter depend on the values of the respiration constants (Appendix Table 1). In the simulation growth respiration accounted for 34% of gross photosynthate production throughout growth, whereas cumulative maintenance respiration increased from 6% at double ridges to 12% at anthesis and 15% at maturity. Figure 6 also illustrates how the dry matter produced is partitioned into the different plant parts. With ARC-WHEAT 1 the functioning of the root submodel does not affect the growth of the plant and the roots are used solely as a sink for assimilate. Further, root data for the six experimental crops are incomplete. For these reasons the effectiveness of the submodel in simulating root growth is not further commented upon. The assimilate pool for grain growth is created at anthesis and thereafter all new assimilate goes to the pool or to the grain. This simulated crop has a grain yield of 8.4 t/ha (9.9 t/ha at 85% moisture content), very similar to that observed, but a harvest index of only 46%, compared with 50% for the observed crop.

Crop simulation using observed leaf areas. These are listed as simulated 1 in Table 1. The closer correspondence is with the late-sown crops. At anthesis these have 2% more top weight than the observed crops and only 3% (43 g/m²) more on average at maturity. Grain yields average 26 g/m² more, most of the difference being for the observed 1981 crop which produced 100 g/m² of grain less than the simulated crop. This is in agreement with

observations made at the time that the 1981 crops did not make as large grain yields as had been expected on the basis of general crop growth.

In contrast to the late-sown crops, the simulations of the early-sown crops overestimated the observed dry-weight gains. Thus, at anthesis the simulated crop weights are 8% greater and at maturity 6% greater. In terms of dry-matter production, the canopies of the early-sown crops may be less efficient at producing dry matter than those of the late-sown, although the observations are rather few on which to base such a claim. The simulated grain yields of the early-sown crops are 6% more than the observed, compared with 3% for the late-sown.

Crop simulation using simulated leaf areas. In these calculations a uniform stand of 250 emerged plants produced tillers and a canopy, as described in more detail by Porter (1984). Table 1 shows that use of the simulated canopies underestimated the dry weight at anthesis of the late-sown crops by 17% but overestimated those of the early-sown by 9%. At maturity these differences are -8 and +19% respectively, and the grain yield differences are -1 and +14%. The least well matched of the six crops is that of 1980E, but in general the use of full simulation does not give as close correspondence, particularly of the late-sown crops, as does the use of observed LAIs in the simulations. The remainder of Table 1 shows the proportions of the grain pool used in the simulations, simulated root weights at anthesis and other components of yield. Components such as number of grains per ear and weight per grain agree quite closely between observed and simulated crops.

Simulation of grain growth. Grain yield is simulated in the model by multiplying the weight per

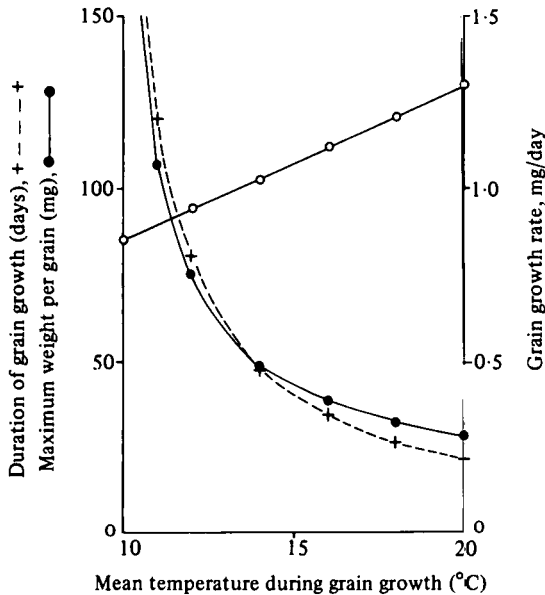


Fig. 7. Illustration of the relationship used in the model between average temperatures during grain growth, grain growth rates, the duration of grain growth and maximum grain weights. Duration of grain growth in days (+---+), maximum grain weight per grain in mg (●—●), and maximum grain growth rates in mg/day (○—○).

grain by the number of grains per square metre. The number of grains per square metre, which is calculated from ear weight at anthesis, is a function of total crop growth and thus of light interception during the ear growth period. The other component of yield, weight per grain, is obtained from the product of the grain growth rate and the duration of grain growth. Carbohydrate for grain growth is supplied either from daily photosynthesis or the pool, and while supplies are adequate growth proceeds at its maximum rate. As shown above, both the maximum grain growth rate and the duration of the grain growth period are functions of temperature and so they and their product are related to the average temperatures of the grain growth period. Figure 7 illustrates this relationship after making the simplifying assumption that the fluctuating temperatures from anthesis to maturity can be adequately represented by single average temperatures. The interval from anthesis to maturity increases asymptotically to infinity as the average temperature falls towards the base temperature of 9 °C, and the grain growth period rises with fall in temperature in a similar fashion. The maximum rate of grain growth falls with mean temperature, but this is more than compensated for by the increase of the duration of the grain-filling period.

The only crop for which detailed measurements of grain weights during grain growth were available was 1981E (G.N. Thorne, personal communication), and grain weights were available for only the four central grains and not for all the grain in the ears. The period of linear grain growth was 37 days and for this the mean temperature was 15.4 °C. Figure 7 shows that a maximum grain weight of 41 mg/grain would be expected. The final observed weight was 37.5 mg/grain, but the detailed observations showed that in this crop the four measured grains reached a maximum weight and then declined, presumably by respiration, by 9%. Thus the average maximum weight for all the grains may have been very close to the value of 41 mg predicted by the grain growth model.

CONCLUSIONS

The simulation of the test crops has shown that it is possible to reproduce quite closely the growth of October-sown crops using observed LAI values, but the use of comparable values for September-sown crops leads to overestimation of dry-matter production. Using the limited published leaf data available it has been possible to reproduce many details of the leaf canopy (Porter, 1984), but simulations of dry-matter production based on such canopies exaggerate the differences observed between September- and October-sown crops and do not reproduce year-to-year fluctuations very well, possibly because of the sensitivity of the simulated canopy to the timing of development stages, particularly anthesis.

During the assessment of these results it has become obvious that improvements can be made to the model in phenological development, canopy structure, respiration, partitioning of assimilate, and ear growth. For some parts, such as canopy structure, new data are already becoming available and the modelling process can be advanced. For other aspects, such as timing of development, there is urgent need for more observations on a range of cultivars and over sites spread throughout the country, especially as this can be used as a practical management tool.

Throughout, the assumption has been made that the growth of the test crop was limited only by temperature and radiation. It is very difficult to determine whether there were unknown constraints present that, had they been removed, would have allowed the same variety to produce more grain in the same year. This is complicated by the fact that the values used for testing the model were obtained from very similar crops. It is important that one of the crops giving the very large yields that are occasionally reported should be observed in some detail, at least from anthesis to harvest. Without

this it will be very difficult to be certain that it was solely temperature and radiation that limited the yields at Rothamsted to 10 t/ha. The power and range of the model thus depends on the data base that it uses. Even at present it is a powerful tool for interpreting observations and pointing to where gaps in knowledge are a limit to understanding.

We thank R. D. Prew and his colleagues for permission to use data from the Rothamsted multi-factorial wheat experiments, and G. N. Thorne for providing unpublished data and giving us valuable advice. We also thank Lynn Parry for computing assistance, J. J. Landsberg for much early planning and inspiration and W. Day for help with the tillering and photosynthesis submodels and valuable discussion and criticism.

REFERENCES

- ARNDT, C. H. (1945). Temperature-growth relationships of the roots and hypocotyls of cotton seedlings. *Plant Physiology* **20**, 200-220.
- AUSTIN, R. B., EDRICH, J. A., FORD, M. A. & BLACKWELL, R. D. (1977). The fate of the dry matter, carbohydrates and ^{14}C lost from the leaves and stems of wheat during grain filling. *Annals of Botany* **41**, 1309-1327.
- CHARLES-EDWARDS, D. A. (1978). An analysis of the photosynthesis and productivity of vegetable crops in the United Kingdom. *Annals of Botany* **42**, 717-731.
- DE WIT, C. T., GOUDRIAAN, J., VAN LAAR, H. H., PENNING DE VRIES, F. W. T., RABBINGE, R. R., VAN KEULEN, H., LOUWERSE, W., SIMBA, L. & DE JONGE, C. (1978). Simulation of assimilation, respiration and transpiration of crops. Pudoc, Wageningen, The Netherlands.
- FRANCIS, C. A. (1970). Effective day-lengths for the study of photo-period sensitive reactions in plants. *Agronomy Journal* **62**, 790-792.
- GALLAGHER, J. N., THORNE, G. N. & TAYLOR, P. J. (1981). Development of winter wheat. *Rothamsted Experimental Station, Report for 1980*. Part 1, pp. 53-54.
- HOCHMAN, Z. (1979). Wheat in a semi-arid environment: a field and simulation study of the effects of water stress on yield. M.Sc. thesis, University of Sydney.
- LANDSBERG, J. J. & PORTER, J. R. (1982). The ARC Wheat Model. In *Aspects of Crop Growth Agronomy Conference* (ed. J. E. Davies and F. E. Shotton). *MAFF Reference Book* 341, pp. 104-115. London: H.M.S.O.
- LUMSDEN, M. E. (1980). The influence of weather on the development of winter wheat. B.Sc. thesis, University of Bath.
- MCCREE, K. J. (1974). Equation for the rate of dark respiration of white clover and grain sorghum, as functions of dry weight, photosynthetic rate, and temperature. *Crop Science* **14**, 509-514.
- MARSHALL, B. & BISCOE, P. V. (1980a). A model for C_3 leaves describing the dependence of net photosynthesis on irradiance. I. Derivation. *Journal of Experimental Botany* **31**, 29-39.
- MARSHALL, B. & BISCOE, P. V. (1980b). A model for C_3 leaves describing the dependence of net photosynthesis on irradiance. II. Application to the analysis of flag leaf photosynthesis. *Journal of Experimental Botany* **31**, 41-48.
- MARTINEZ-CARRASCO, R. & THORNE, G. N. (1979). Effects of crop thinning and reduced grain numbers per ear on grain size in two winter wheat varieties given different amounts of nitrogen. *Annals of Applied Biology* **92**, 383-393.
- MILTHORPE, F. L. & MOORBY, J. (1979). *An Introduction to Crop Physiology*. Cambridge: Cambridge University Press.
- MORGAN, J. M. (1976). A simulation model of the growth of the wheat plant. Ph.D. thesis, Macquarie University.
- PEARMAN, I., THOMAS, S. M. & THORNE, G. N. (1977). Effects of nitrogen fertilizer on growth and yield of spring wheat. *Annals of Botany* **41**, 93-108.
- PENNING DE VRIES, F. W. T. & VAN LAAR, H. H. (ed.) (1982). *Simulation of Plant Growth and Crop Production*. Pudoc, Wageningen, The Netherlands.
- PORTER, J. R. (1984). A model of canopy development in winter wheat. *Journal of Agricultural Science, Cambridge* **102**, 383-392.
- PORTER, J. R., BRAGG, P. L., RAYNER, J. H., WEIR, A. H. & LANDSBERG, J. J. (1983). The ARC wheat simulation model - principles and progress. In *Opportunities for Manipulations of Cereal Productivity* (ed. A. Hawkins and B. Jeffcoat). *British Plant Growth Regulator Group, Monograph* **7**, pp. 97-108.
- PREW, R. D., CHURCH, B. M., DEWAR, A. M., LACEY, J., PENNY, A., PLUMB, R. T., THORNE, G. N., TODD, A. D. & WILLIAMS, T. D. (1983). Effects of eight factors on the growth and nutrient uptake of winter wheat and on the incidence of pests and diseases. *Journal of Agricultural Science, Cambridge* **100**, 363-382.
- SPIERTZ, J. H. J. (1977). The influence of temperature and light intensity on grain growth in relation to the carbohydrate and nitrogen economy of the wheat plant. *Netherlands Journal of Agricultural Science* **25**, 182-197.
- TENHUNEN, J. D., WEBER, J. A., YOCUM, C. S. & GATES, D. M. (1976). Development of a photosynthesis model with an emphasis on ecological applications. II. Analysis of a data set describing the P_M surface. *Oecologia* **26**, 101-119.
- TENHUNEN, J. D., YOCUM, C. S. & GATES, D. M. (1976). Development of a photosynthesis model with an emphasis on ecological applications. I. Theory. *Oecologia* **26**, 89-100.
- THORNE, G. N., DEWAR, A. M., WILLIAMS, T. D., LACEY, J., PLUMB, R. T., PREW, R. D., CHURCH, B. M. & TODD, A. D. (1982). Factors limiting yield of winter

- wheat. *Rothamsted Experimental Station, Report for 1980*, Part 1, pp. 19–20.
- THORNE, G. N., DEWAR, A. M., WILLIAMS, T. D., LACEY, J., PLUMB, R. T., PREW, R. D., PENNY, A., CHURCH, B. M. & TODD, A. D. (1981). Factors limiting yield of winter wheat. *Rothamsted Experimental Station, Report for 1981*, Part 1, p. 18.
- THORNLEY, J. H. M. (1976). *Mathematical Models in Plant Physiology*. London and New York: Academic Press.

Appendix Table 1. *Parameter values*

Phenological development		Base temperature (°C)	Thermal time	
Sowing to emergence		1	148 °C days	
Emergence to double ridge		1	284 FV × FP × °C days	
Double ridge to anthesis		1	600 FP × °C days	
Anthesis to maturity		9	350 °C days	
PAR interception				
Extinction coefficient, <i>k</i>			0.44	
Leaf transmission coefficient, <i>m</i>			0.10	
Photosynthesis				
Photosynthetic efficiency, α			0.009 mg/J	
Ambient CO ₂ concentration, <i>C_a</i>			600 mg/m ³	
Boundary layer resistance, <i>r_a</i>			30 sec/m	
Mesophyll resistance, <i>r_m</i>			400 sec/m	
Activation energy of the electron transport system, ΔH_1			14 200 cal/mol	
Denaturation energy of the electron transport system, ΔH_2			47 000 cal/mol	
Entropy change on denaturation of the electron transport system, ΔS			153.4 cal/K per mol	
Gas constant, <i>R</i>			1.987 cal/K per mol	
Respiration				
Growth respiration coefficient, <i>a</i>			0.34	
Maintenance respiration coefficient, <i>b</i> :				
Emerge to anthesis			0.002	
Anthesis to maturity			0.001	
Dry-matter partitioning				
	Proportions of current assimilate			
	Roots	Leaves	Stems	Ears
Emergence to double ridge	0.35	0.55	0.10	0
Double ridge to beginning ear growth	0.20	0.40	0.40	0
Beginning ear growth to anthesis	0.10	0.30	0.30	0.30